European Congress on Computational Methods
in Applied Sciences and Engineering (ECCOMAS 2012)
J. Eberhardsteiner et.al. (eds.)
Vienna, Austria, September 10-14, 2012

A FRACTURE MODEL FOR PEARLITIC STEEL BARS USING A COHESIVE MODEL

F. Suárez[1], J.C. Gálvez[1], D.A. Cendón[2], J.M. Atienza[2] and M. Elices[2]

[1] Departamento de Ingeniería Civil-Construcción, Universidad Politécnica de Madrid
E.T.S.I. Caminos, Canales y Puertos, C/Profesor Aranguren s/n 28040 – Madrid, Spain
e-mail: fsuarez@caminos.upm.es; jaime.galvez@upm.es

[2] Departamento de Ciencia de Materiales, Universidad Politécnica de Madrid
E.T.S.I. Caminos, Canales y Puertos, C/Profesor Aranguren s/n 28040 – Madrid, Spain
e-mail: dcendon@mater.upm.es; jmatienza@mater.upm.es; melices@mater.upm.es

Keywords: tensile, test, cohesive model, fracture, steel, triaxiality

Abstract. *The fracture of ductile materials, such as metals, is usually explained with the theory of nucleation, growth and coalescence of microvoids. Based on this theory, many numerical models have been developed, with a special mention to Gurson-type models. These models simulate mathematically the physical growth of microvoids, leading to a progressive development of the internal damage that takes place during a tensile test. In these models, the damage starts to develop in very early stages of the test.*

Tests carried out by the authors suggest that, in the case of some eutectoid steels such as those used for manufacturing prestressing steel wires, the internal damage that takes place as a result of the growth of microvoids is only noticeable in very late stages of the tensile test.

In the authors' opinion, using a cohesive model as a failure criterion may be interesting in this case; a cohesive model only requires two parameters to be defined, with the fracture energy being one of them, which can be obtained experimentally. In addition to this, given that it is known that the stress triaxiality has a strong influence on the fracture of ductile materials, a cohesive model whose parameters are affected by the value of the stress triaxiality can be considered.

This work presents a fracture model for steel specimens in a tensile test, based on a cohesive behaviour and taking into account the effect of stress triaxiality, which is different at each point of the fracture plane.

1 INTRODUCTION

The fracture of ductile materials has usually been explained with the theory of nucleation, growth and coalescence of microvoids. According to this theory, at a first stage and with a high loading being applied, microvoids are developed inside the material (nucleation) due to a decohesive process of small inclusions that are torn apart from the rest of the material or by the fracture of the particle that constitutes the inclusion itself. At a second stage, and under higher deformational states, these microvoids increase their size (growth) until they finally become interconnected (coalescence). Such a process weakens the material until its eventual failure.

This theory has been the basis of several numerical models that have sought to reproduce the fracture on ductile materials, with the Gurson model being the most popular of them [1]. Since its appearance, this type of models has been successfully applied to different ductile materials, such as aluminium, copper or steel. Subsequent evolutions of the Gurson model have been able to reproduce, not only the softening due to the growth of microvoids, but also the eventual fracture of the material [2].

As already mentioned, these models are based on the theory of nucleation, growth and coalescence of microvoids; an evidence of this physical process can be observed, for instance, on the fracture surface that results from a tensile test carried out on a cylindrical specimen of pearlitic steel, used for manufacturing prestressing steel wires (see Figure 1). As shown in [3], the central dark region is the result of a process of nucleation and growth of microvoids, which damages the specimen, just like the Gurson model estates, until it finally causes the specimen to fail.

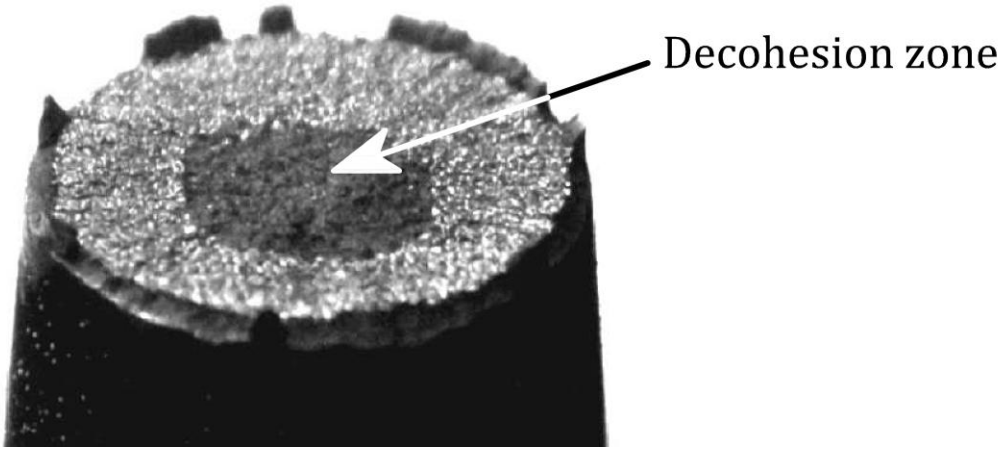

Figure 1: Fracture surface of one of the specimens tested

Even though the Gurson-type models reproduce the physical process that leads to the eventual failure of the material, they present certain disadvantages, especially the large number or parameters needed as input and the fact that these parameters are not measurable by means of experimental testing, since they are based on values such as the volume of voids contained in the material when the coalescence starts or the volume of voids needed for the material to fail.

On another note, according to some research it seems that the stress triaxiality state (σ_H/σ_{VM}) plays an important role on the mechanisms that lead to the failure of a ductile

material such as steel [4]. In fact, the Gurson model formulation includes σ_H and σ_{VM}, which means that the stress triaxiality is considered as a key factor in the damaging process.

In this paper, an alternative to Gurson-type models is presented, a cohesive model that has been applied to reproduce the failure on pearlitic steel, used for manufacturing prestressing steel wires. The use of such a cohesive model as a failure mechanism enables easier calibration, since it only requires two parameters, f_t and G_F, with the latter being obtainable experimentally. Unlike traditional cohesive crack models [5], the one presented in this paper includes the stress triaxiality as a key factor that modifies the cohesive behaviour of the material.

2 EXPERIMENTAL WORK

The main purpose of the following experimental work is to identify, in the loading-strain curve (F-ε diagram), the moment at which the internal damage that leads to the eventual failure begins. To this end, two different groups of tests are developed, with the first one consisting of tensile tests carried out until failure and with the second one consisting of tensile tests stopped just before failure.

As a result of the first group of tests, the F-ε diagram could be defined with high accuracy. This was necessary so that the tests carried out in the second group could be stopped at certain points of the curve and, as an eventual result, the appearance of the internal damage could be delimited.

2.1 Material

In the manufacturing process to obtain steel wires, raw eutectoid steel bars are cold-drawn, reducing their section by pulling it through a conical die. For this research, specimens were obtained from raw eutectoid pearlitic steel bars used for manufacturing prestressing steel wires, that is to say, they had not been affected by cold-drawing so the material was as isotropic as possible.

2.2 Specimens

The specimens tested were cylindrical and with a diameter of 6mm. The dimensions can be checked in Figure 2.

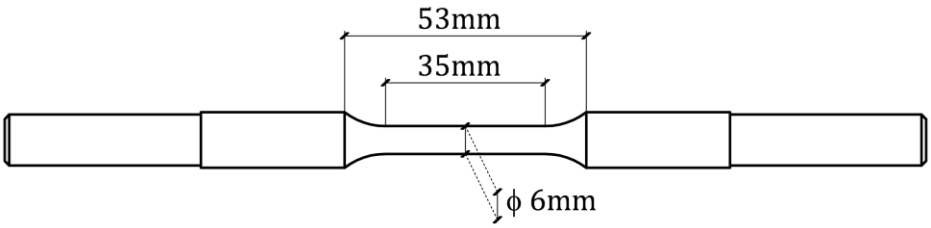

Figure 2: Specimen dimensions

2.3 Tensile tests

-Tests carried out until failure

As previously mentioned, at a first stage three specimens were tested in order to obtain the F-ε diagram, which is shown in Figure 3.

-Tests stopped before failure

Once the F-ε diagram was completely defined, two specimens were tested and stopped before failure at certain points of the diagram, but in particular at loading values of 29kN and 28.5kN, as shown in Figure 3.

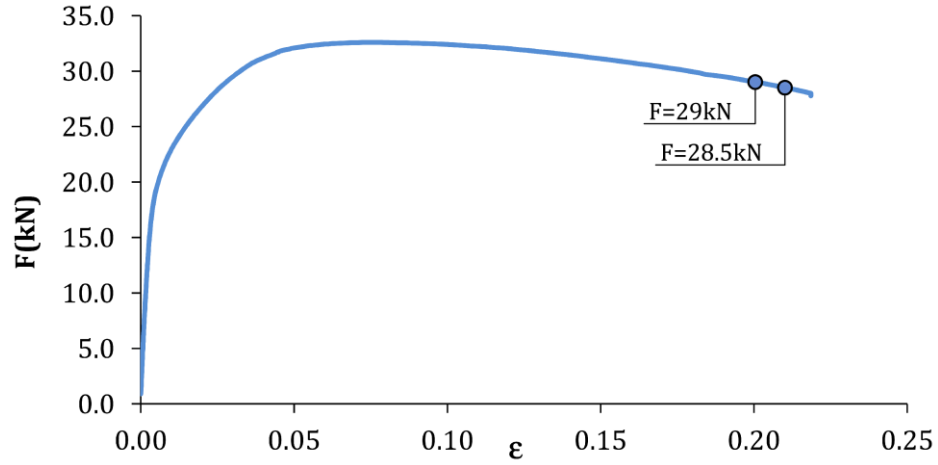

Figure 3: F-ε diagram. Blue circles point out the moments at which the tests were stopped for each of the specimens tested.

The specimen corresponding to the test carried out to a higher deformational state stopped at a loading value of 28.5kN, was also analysed by means of X-ray computed tomography (Nanotom 160NF, Phoenix), in order to check the dimension of the internal damage developed. In principle, X-ray tomography allows detection of existing internal damage in the specimen, but only when thin specimens are analysed. This technique was applied in order to check if it could be applied with 6mm-diameter specimens. These results were obtained with the collaboration of IMDEA Materiales.

Finally, both specimens were tested until failure at very low temperature with an accelerated tensile test; the test was performed by submerging the specimens in liquid nitrogen and applying a rapid displacement of the clamping jaws. This procedure leads to an embrittled fracture that allows appreciation of the internal damage developed before the accelerated test without introducing additional damage. During these tests the temperature was measured using a thermocouple, as shown in Figure 4.

2.4 Results

Figure 5 shows the fracture surface of each specimen after the accelerated tensile test carried out with liquid nitrogen. In the case of the test stopped at 29kN no trace of damage to the specimen could be observed on its failure surface, whereas in the case of the test stopped at 28.5kN a small circular shaped dark area was visible after the embrittled fracture test (see Figure 5).

The tomography obtained for the specimen whose initial test was carried out to a higher deformational state (F=28.5kN) showed internal damage very similar to the damage observed after the embrittled fracture caused with the accelerated tensile test described before. A comparison between each one, the tomography and the fracture surface after the embrittled fracture, can be observed in Figure 6.

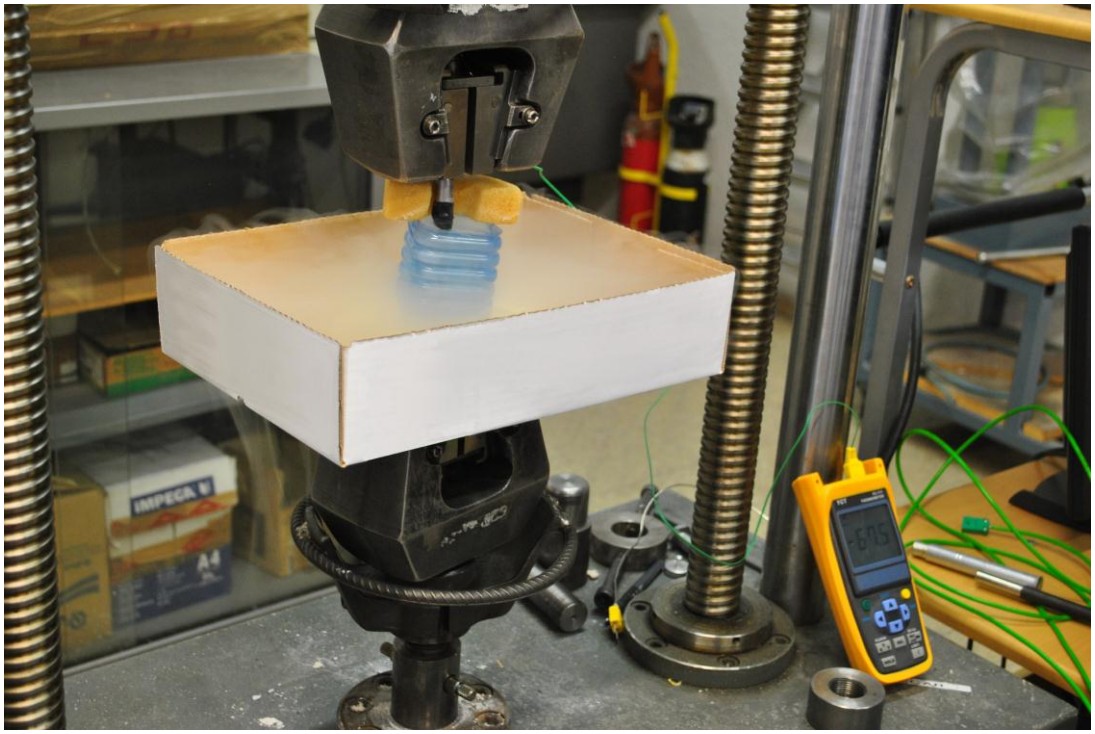

Figure 4: Accelerated tensile test. Specimens were submerged in liquid nitrogen and the temperature measured with a thermocouple.

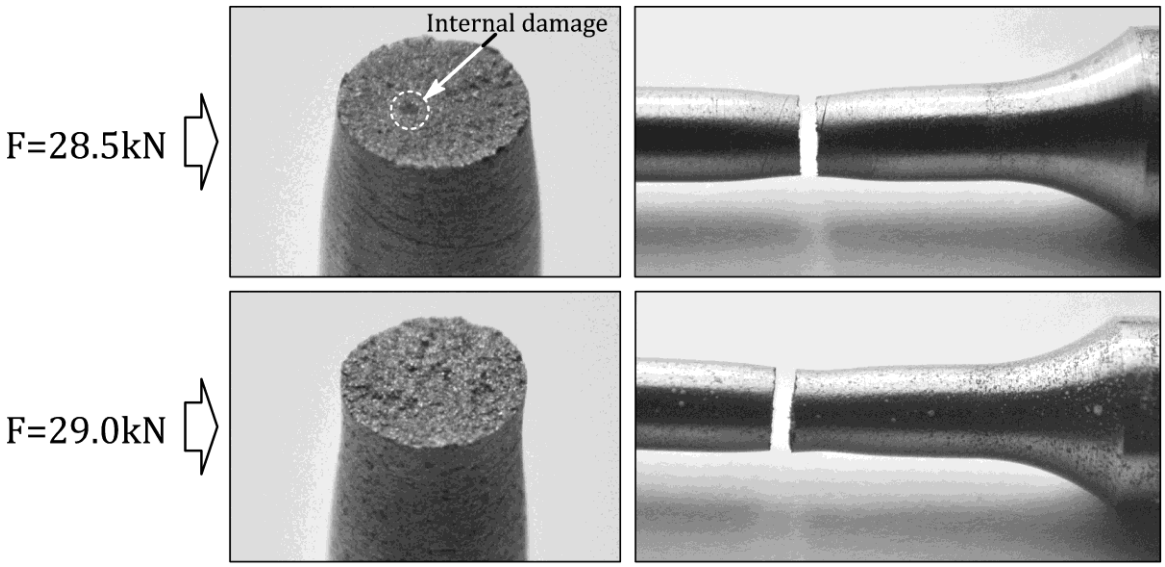

Figure 5: Fracture surfaces of the specimens after the accelerated tensile test, with the specimens submerged in liquid nitrogen.

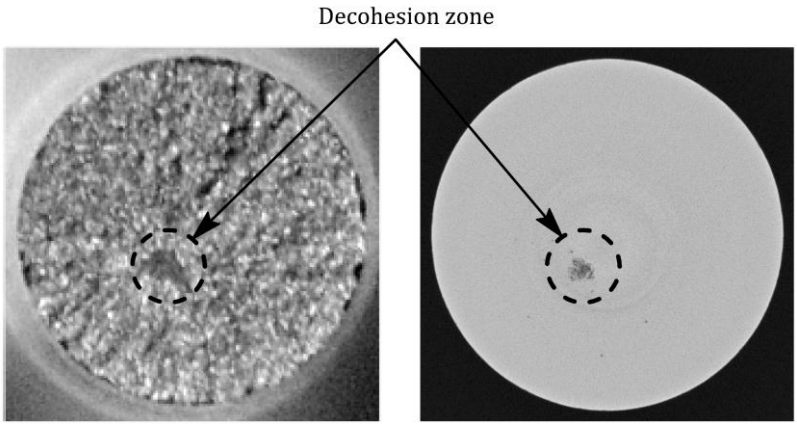

Figure 6: Internal damage observed for the specimen whose test was stopped at F=28.5kN: a) Fracture surface after the accelerated test, b) Image obtained by X-ray tomography before the accelerated test.

The tested to a lower deformational state (F=29kN) did not fail at the smaller section, as expected. Apparently, if the internal damage had already started to develop, it was not big enough to cause the failure of the specimen.

According to these results, the internal damage seems to develop in the very last part of the F-ε curve, between the points shown in Figure 3.

3 COHESIVE INTERFACE ELEMENT DEPENDENT ON THE STRESS TRIAXIALITY

In this section, the interface element developed is described. Whilst a traditional cohesive element behaviour [5] is defined only by the fracture energy (G_F) and the decohesion stress (f_t), this element allows simulation of the fracture process in a defined plane with a cohesive behaviour affected by the stress triaxiality value in every element of the model.

This element was developed in ABAQUS, using a UEL user subroutine.

3.1 Decohesion plane

The element has been programmed to reproduce decohesion on the YZ plane. The interface element is a rectangular element placed on the YZ plane, with nodes that also define the face of a brick element that is part of the specimen. As the tensile test is developed along the X axis, the tension forces are perpendicularly applied to the interface element plane.

Decohesion starts when σ_{xx} reaches a value equal to the decohesion stress f_t. Figure 7 shows a sketch of the interface element and the brick element connected to it.

3.2 Large strains

Due to the elastic-plastic behaviour of steel, the element is programmed to take into account the effect of large strains, this is to say, the area reduction that takes place as a result of the deformation of the brick element to which it is connected. Under the assumption of constant volume, tensile loading stretches the brick element along the X axis, causing its sectional area to reduce, as shown in Figure 8.

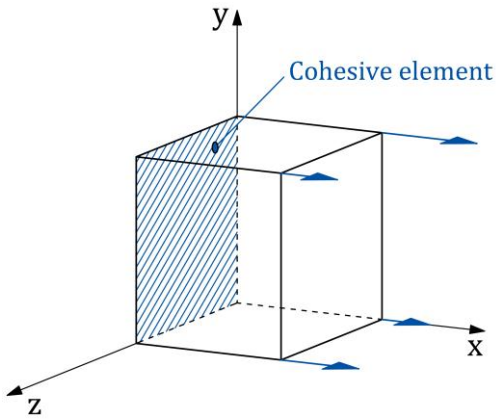

Figure 7: The tensile test is simulated to develop along the X axis, perpendicularly to the interface element plane.

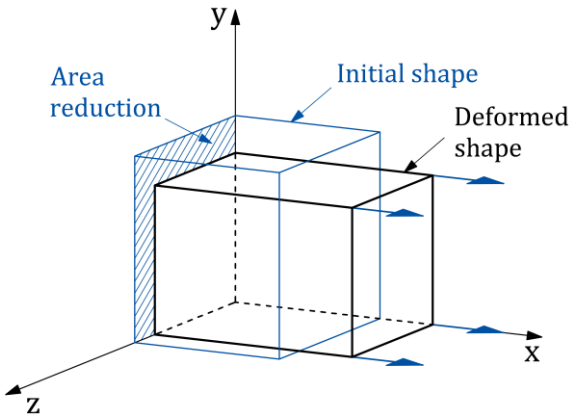

Figure 8: Large strains lead to a reduction of the cross-sectional area of the brick element and, therefore, to a change of shape of the interface element.

In each time step during the calculation process, the Jacobian matrix of each interface element is updated, using the nodal coordinates resulting from the previous step. Nodal coordinates are also updated for each time step.

3.3 The softening curve

The softening curve has been adapted to represent the plastic behaviour of steel. According to Dugdale [6], decohesion process for steel can be reproduced by using a rectangular curve. In this work, a smooth and therefore more realistic variant of Dugdale's rectangular softening curve is proposed. In this alternative softening curve stress progressively decreases, with it being slow at the beginning and fast in the last part of the curve. In particular, the softening curve used in this study is defined by using an equation of the following kind: $y=A-B\cdot x^2$, resulting in the softening curve shown in Figure 9.

3.4 The role of the stress triaxiality

The softening curve is defined by the fracture energy (G_F) and the decohesion stress (f_t). These parameters are defined as dependent on the stress triaxiality value (σ_H/σ_{VM}) in the brick element to which the interface cohesive element is connected. Therefore, initial values of G_F and f_t must be set as input and then, during the calculation process, are modified by a factor that depends on the stress triaxiality, as shown in Figure 10. The initial value of G_F is divided by this factor while the initial value of f_t is multiplied by it. It is acknowledged that this approach is not new, a similar one can be found in the work by Siegmund and Brocks [7].

Figure 11 describes how the subroutine works. The cohesive element is an interface flat element, whose nodes also define one of the faces of the brick element to which it is connected. Given that decohesion takes place on the YZ plane, the cohesive element must be contained on that plane. During the calculation process, for every time step in which it is divided, the user subroutine obtains the von Mises stress and the hydrostatic stress of the brick element connected to the cohesive element. Once the stress triaxiality is obtained, the values of the parameters that define the softening curve, G_F and f_t, are recalculated.

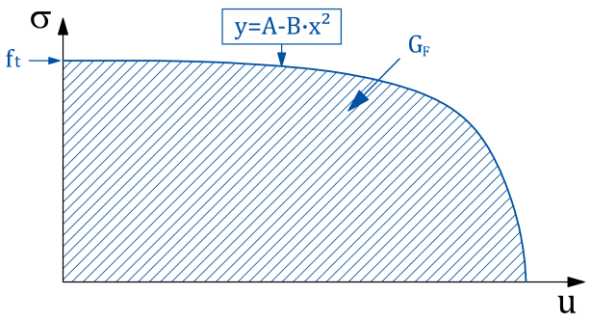

Figure 9: The softening curve used in the numerical model.

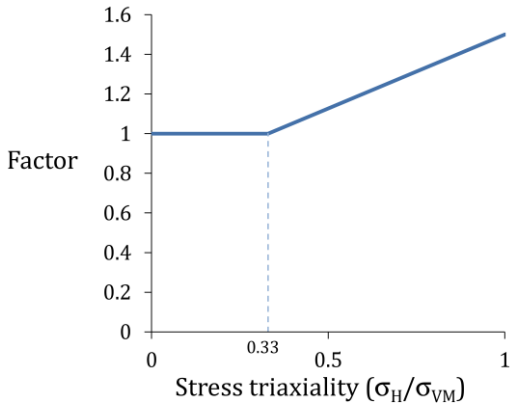

Figure 10: The correction factor depends on the stress triaxiality value, according to this function.

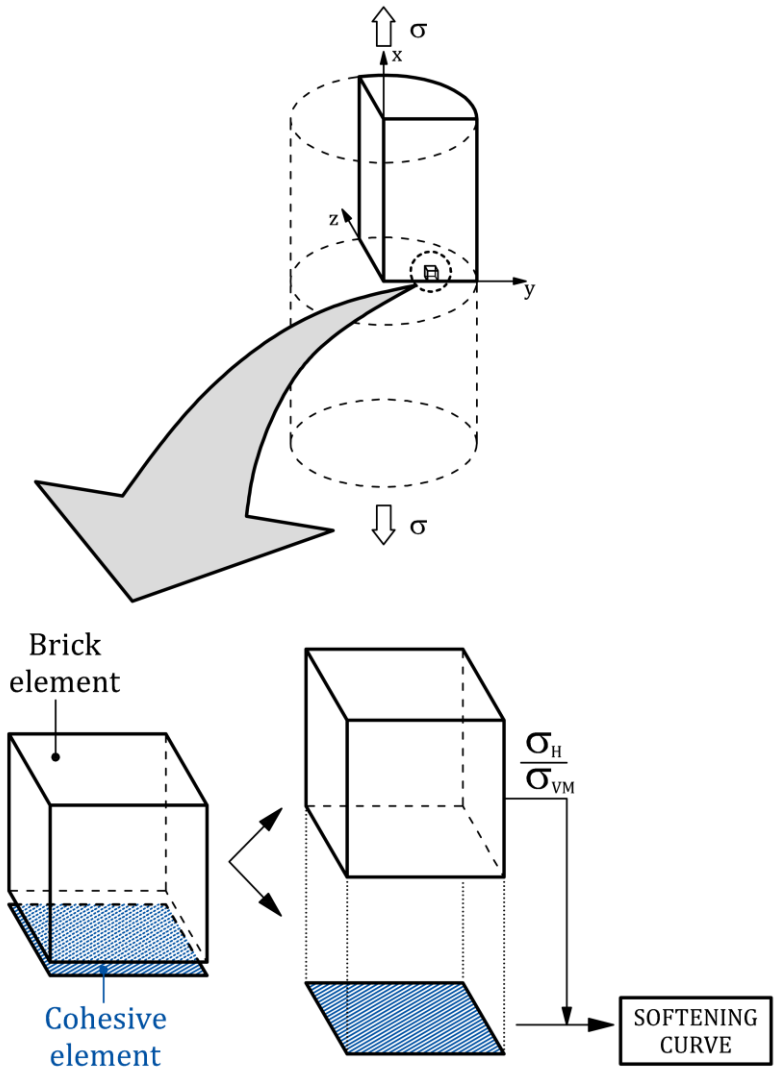

Figure 11: Graphical representation of the calculation process in a time step for a cohesive element.

4 NUMERICAL SIMULATION

The interface element described in the previous section was used to simulate a tensile test on a 6mm diameter specimen. Only an eighth part of the specimen was modelled, with the YZ plane being the fracture plane. Figure 12 shows a picture of this model.

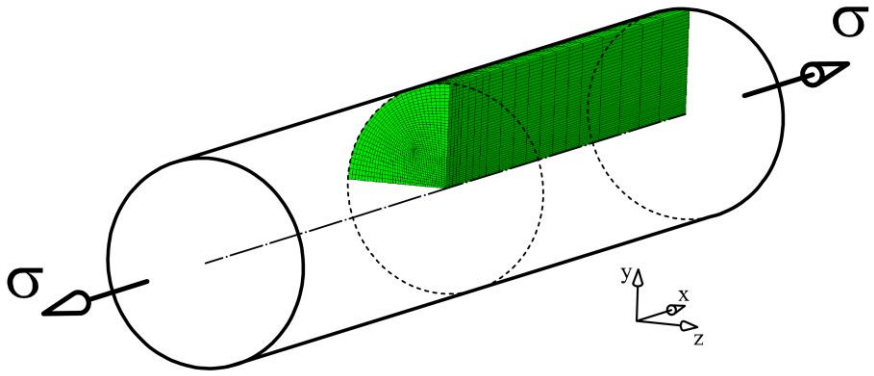

Figure 12: Finite element mesh used in the numerical simulation.

Simulations were run with ABAQUS 6.9 and the interface element, as mentioned formerly, was developed with a UEL user subroutine.

Unlike other models based on the Gurson model, this one only requires adjustment of the parameters of a cohesive model, that is to say, the decohesion stress (f_t) and the fracture energy (G_F), which can be experimentally obtained with a three-point bending test.

4.1 Material

The calculation was made under the assumption of large strains and the von Mises yield criterion used in the brick elements. The material behaviour was defined by the σ-ε curve obtained experimentally before the maximum loading point; the rest of the curve was calibrated with the experimental results. The fracture behaviour was implemented by using a softening curve defined by the fracture energy, measured by means a three-point bending test, and the decohesion stress, which was calibrated with the curves obtained experimentally.

4.2 Loading

Loading was applied by imposing a displacement on the specimen end placed further from the decohesion plane.

4.3 Simulation of fracture

At a certain point of the test, the specimen begins to neck, which leads to a stress concentration in the centre of the future fracture plane. When the interface element connected to the brick element placed in the centre of the specimen reaches a value of σ_{xx} equal to f_t, the decohesion process begins in this element. Such decohesion unloads the central brick element and loads up the elements around it. Therefore, fracture propagates from inside to outside.

The images in Figure 13 show how the decohesion process propagates in the numerical simulation. It should be noted that strains in the direction of the X axis have been magnified by a factor of 100 in order to make them more noticeable.

On the curve obtained numerically, a circle shows the beginning of the decohesion process.

The numerically-obtained curve fits reasonably well with the one obtained experimentally. In addition to this, the decohesion process, which simulates the internal damage observed on the fracture surface of the specimens tested, starts at the very last part of the curve. These results seem to agree with the experimental results obtained with the X-ray tomography.

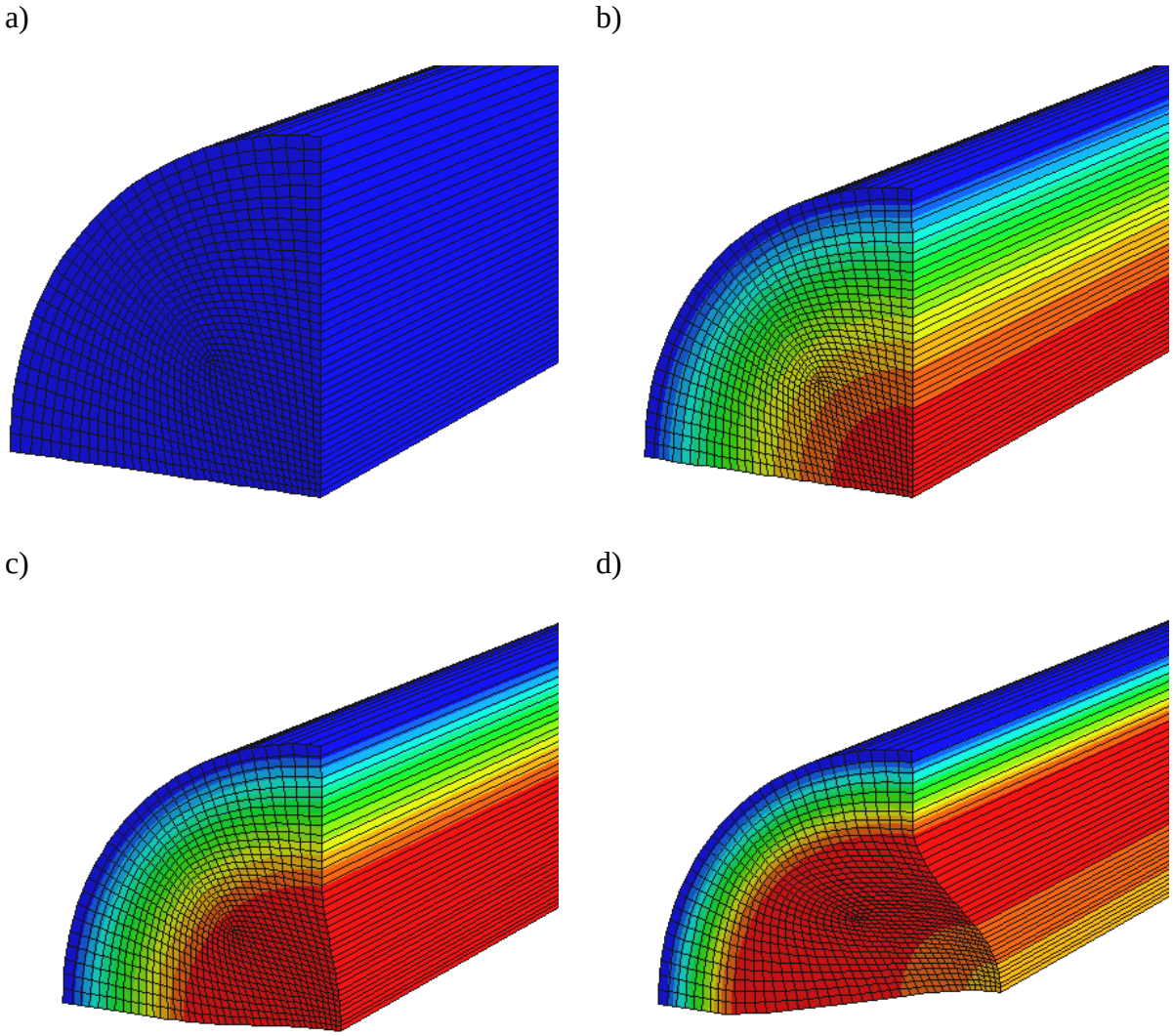

Figure 13: Damage evolution. Note: strain in the direction of the X axis are affected by a factor of 100: a) Before loading; b) Stress concentration at the specimen axis; c) Decohesion process begins in the centre of the specimen; d) Decohesion propagates from inside to outside.

5 RESULTS

5.1 The loading-strain curve

F-ε curve obtained experimentally is compared to that obtained with the numerical simulation in Figure 14. To allow comparison in the numerical simulation the strain is measured using a reference point placed at 6.25mm from the fracture plane, exactly the distance corresponding to half the extensometric base length.

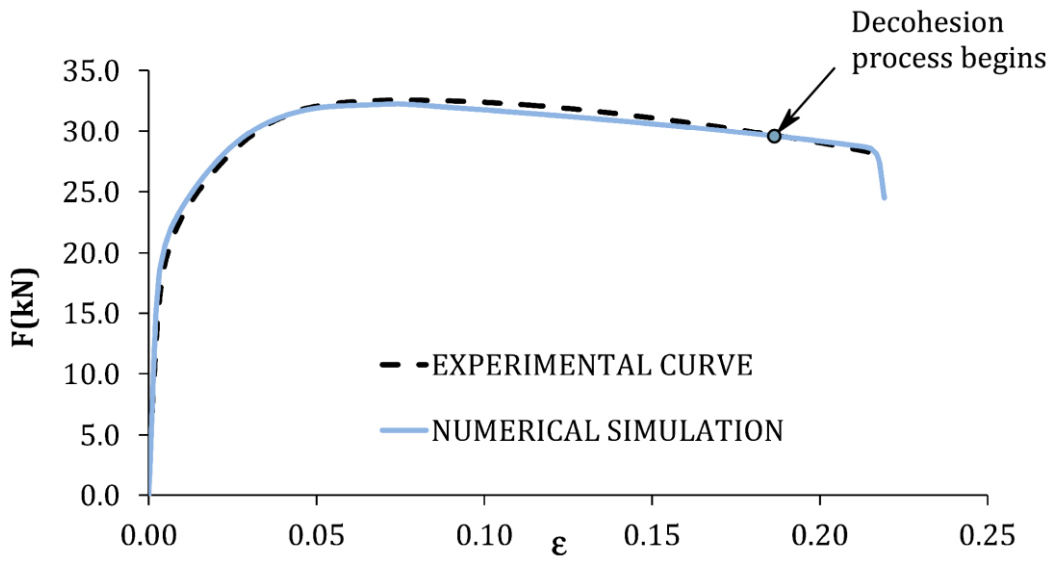

Figure 14: F-ε curves obtained experimentally and numerically.

6 CONCLUSIONS

The preliminary results presented in this paper suggest that the internal damage observed on cylindrical specimens of pearlitic steel, identified by a dark region on the fracture surface, is developed in the last moments of a tensile test.

In this study a cohesive model dependent on the stress triaxiality state of the elements has been presented. The model was implemented with ABAQUS using a UEL user subroutine and simulates the fracture of a cylindrical specimen starting in the centre of the fracture section and propagating outwards. As observed experimentally, numerically-simulated fracture takes place in the last moments of the tensile test.

As already mentioned, this paper presents previous results of a more extensive study, focused on the behaviour of steel in the last region of the F-ε curve, from the moment of maximum load to the eventual fracture of the material. To date, the most widely extended numerical models have been those based on the Gurson-Tvergaard-Needleman approach [2] that, although solidly proven from the numerical point of view, require a high number of parameters to be calibrated (which cannot be experimentally measured). Hence, the main advantage of a cohesive model is that it needs a lower number of parameters to be defined, of which some can be measured experimentally.

ACKNOWLEDGEMENTS

The authors gratefully acknowledge the financial support provided for this research by the Spanish Ministerio de Economía y Competitividad under grant DPI 2011-24876 and IPT-420000-2010-31.

They also express their gratitude to Jon Molina-Aldareguia and Federico Sket, from Instituto IMDEA Materiales, for their invaluable aid with the X-ray tomographic analysis and Luis del Pozo and Luisa Villares, from Emesa Trefilería, S.A. (Arteixo, La Coruña) for supplying the steel wires, as well as for providing their useful comments.

Finally, F. Suárez also wishes to express his gratitude to the Fundación Agustín de Betancourt for the grant provided.

REFERENCES

[1] Gurson, A.L.: Continuum Theory of Ductile Rupture by Void Nucleation and Growth: Part I – Yield Criteria and Flow Rules for Porous Ductile Media, *J. Eng. Mater. Tech.* (January 1977)

[2] Tvergaard, V., Needleman, A., Analysis of the cup-cone fracture in a round tensile bar, *Acta metall.* Vol. 32, No. 1, pp. 157-169 (1984).

[3] Suárez F., Cendón D.A., Atienza J.M., Gálvez J.C., Elices M., Análisis de la deformación de rotura en el ensayo de tracción en probetas cilíndricas de acero perlítico, *Anales de Mecánica de la Fractura*, 28, Vol. I, pp.205-210 (2011).

[4] Bao Y., Wierzbicki T., On fracture locus in the equivalent strain and stress triaxiality space, *Int. J. Mech. Sci.* 46, pp. 81-98 (2004).

[5] Bazant Z.P., Planas J., Fracture and size effect in concrete and other quasibrittle materials, CRC Press, Boca Raton, FL (1998).

[6] Dugdale D.S., Yielding of steel sheets containing slits, *Journal of Mechanics and Physics of Solids*. 8, pp.100-108 (1960).

[7] Siegmund T., Brocks W., A numerical study on the correlation between the work of separation and the dissipation rate in ductile fracture, *Eng. Fract. Mech*. 67, pp.139-154 (2000).